J | A | C | S
JOURNAL OF THE AMERICAN CHEMICAL SOCIETY

Article

Mixed Quantum Mechanical/Molecular Mechanical (QM/MM) Study of the Deacylation Reaction in a Penicillin Binding Protein (PBP) versus in a Class C β-Lactamase

Benjamin F. Gherman, Shalom D. Goldberg, Virginia W. Cornish, and Richard A. Friesner

J. Am. Chem. Soc., **2004**, 126 (24), 7652-7664• DOI: 10.1021/ja036879a • Publication Date (Web): 28 May 2004

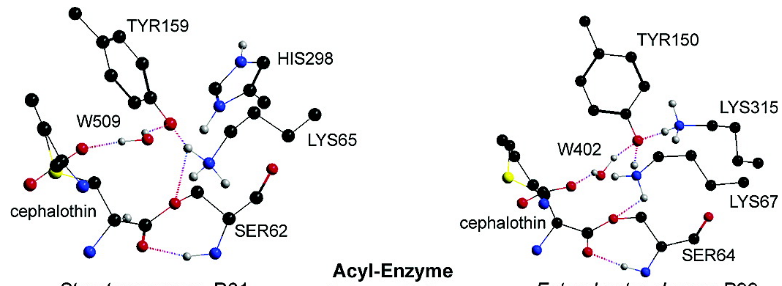

Streptomyces sp. R61 penicillin-binding protein

Acyl-Enzyme Intermediates

Enterobacter cloacae P99 class C β-lactamase

J|A|C|S
ARTICLES
Published on Web 05/28/2004

Mixed Quantum Mechanical/Molecular Mechanical (QM/MM) Study of the Deacylation Reaction in a Penicillin Binding Protein (PBP) versus in a Class C β-Lactamase

Benjamin F. Gherman, Shalom D. Goldberg, Virginia W. Cornish, and Richard A. Friesner*

Contribution from the Department of Chemistry and Center for Biomolecular Simulation, Columbia University, New York, New York 10027

Received June 24, 2003; E-mail: rich@chem.columbia.edu

Abstract: The origin of the substantial difference in deacylation rates for acyl-enzyme intermediates in penicillin-binding proteins (PBPs) and β-lactamases has remained an unsolved puzzle whose solution is of great importance to understanding bacterial antibiotic resistance. In this work, accurate, large-scale mixed ab initio quantum mechanical/molecular mechanical (QM/MM) calculations have been used to study the hydrolysis of acyl-enzyme intermediates formed between cephalothin and the DD-peptidase of *Streptomyces* sp. R61, a PBP, and the *Enterobacter cloacae* P99 cephalosporinase, a class C β-lactamase. Qualitative and, in the case of P99, quantitative agreement was achieved with experimental kinetics. The faster rate of deacylation in the β-lactamase is attributed to a more favorable electrostatic environment around Tyr150 in P99 (as compared to that for Tyr159 in R61) which facilitates this residue's function as the general base. This is found to be in large part accomplished by the ability of P99 to covalently bind the ligand without concurrent elimination of hydrogen bonds to Tyr150, which proves not to be the case with Tyr159 in R61. This work provides an essential foundation for further work in this area, such as selecting mutations capable of converting the PBP into a β-lactamase.

I. Introduction

In the past decade, antibiotic resistance has emerged as a major health care problem.[1−8] β-Lactam antibiotics (e.g., penicillins and cephalosporins) are among the most common drugs currently prescribed to treat bacterial infections.[9,10] These antibiotics work by covalently binding to the active site of D-alanyl-D-alanine carboxy-peptidase/transpeptidase enzymes (also known as penicillin-binding proteins, or PBPs) that catalyze the biosynthesis of bacterial cell wall peptidoglycan, thereby preventing assembly of the bacterial cell wall and resulting in cell death.[10−13] Resistance to these antibiotics is conferred principally via β-lactamases, which bind the antibiotics in a similar fashion but are then able to rapidly hydrolyze the substrate, thus destroying the antibiotic agent and regenerating the enzyme to enable breakdown of further antibiotic molecules.[14−17]

Both PBPs and β-lactamases are serine-protease type enzymes that form an acyl-enzyme intermediate with the substrate.[18,19] But while β-lactamases efficiently catalyze hydrolysis of the acyl-enzyme intermediate, PBPs are very poor catalysts of this hydrolysis reaction and so are effectively trapped as the acyl-enzyme intermediate and inactivated. Our studies focus on the DD-peptidase of *Streptomyces* sp. R61 (hereafter named R61)[20,21] and the *Enterobacter cloacae* P99 cephalosporinase (hereafter named P99),[22,23] two of the most well characterized PBPs and β-lactamases, respectively. The difference in activity between these two proteins illustrates the complexity of enzyme catalysis and the difficulty of protein design. Although there is only a moderate degree of sequence homology (21%), the three-dimensional structures of the two proteins are very similar[20,22] and many of the critical active site residues are conserved.[24] Yet, depending on the substrate, the rate constant for hydrolysis

(1) Cohen, M. L. *Science* **1992**, *257*, 1050−1055.
(2) Neu, H. C. *Science* **1992**, *257*, 1064−1073.
(3) Levy, S. B. *Sci. Am.* **1998**, *278*, 46−53.
(4) Davies, J. *Science* **1994**, *264*, 375−382.
(5) Bush, K.; Jacoby, G. A.; Medeiros, A. A. *Antimicrob. Agents Chemother.* **1995**, *39*, 1211−1233.
(6) Walsh, C. *Nature* **2000**, *406*, 775−781.
(7) Normark, B. H.; Normark, S. *J. Intern. Med.* **2002**, *252*, 91−106.
(8) Bradford, P. A. *Clin. Microbiol. Rev.* **2001**, *14*, 933−951.
(9) Demain, A. L.; Elander, R. P. *Antonie Van Leeuwenhoek* **1999**, *75*, 5−19.
(10) Frère, J. M.; Joris, B. *Crit. Rev. Microbiol.* **1985**, *11*, 299−396.
(11) Waxman, D. J.; Strominger, J. L. *Annu. Rev. Biochem.* **1983**, *52*, 825−869.
(12) Ghuysen, J.-M. *Trends Microbiol.* **1994**, *2*, 372−380.
(13) Ghuysen, J.-M. *Int. J. Antimicrob. Agents* **1997**, *8*, 45−60.
(14) Knotthunziker, V.; Petursson, S.; Waley, S. G.; Jaurin, B.; Grundstrom, T. *Biochem. J.* **1982**, *207*, 315−322.
(15) Frère, J. M. *Mol. Microbiol.* **1995**, *16*, 385−395.
(16) Knox, J. R.; Moews, P. C.; Frère, J. M. *Chem. Biol.* **1996**, *3*, 937−947.
(17) Pratt, R. F. *J. Chem. Soc.-Perkin Trans. 2* **2002**, 851−861.
(18) Ghuysen, J.-M. *Annu. Rev. Microbiol.* **1991**, *45*, 37−67.
(19) Joris, B.; Ghuysen, J.-M.; Dive, G.; Renard, A.; Dideberg, O.; Charlier, P.; Frère, J. M.; Kelly, J. A.; Boyington, J. C.; Moews, P. C.; Knox, J. R. *Biochem. J.* **1988**, *250*, 313−324.
(20) Kelly, J. A.; Knox, J. R.; Zhao, H. C.; Frère, J. M.; Ghuysen, J.-M. *J. Mol. Biol.* **1989**, *209*, 281−295.
(21) Kelly, J. A.; Kuzin, A. P. *J. Mol. Biol.* **1995**, *254*, 223−236.
(22) Lobkovsky, E.; Moews, P. C.; Liu, H. S.; Zhao, H. C.; Frère, J. M.; Knox, J. R. *Proc. Natl. Acad. Sci. U.S.A.* **1993**, *90*, 11 257−11 261.
(23) Crichlow, G. V.; Kuzin, A. P.; Nukaga, M.; Mayama, K.; Sawai, T.; Knox, J. R. *Biochemistry* **1999**, *38*, 10 256−10 261.

10.1021/ja036879a CCC: $27.50

of the acyl-enzyme intermediate differs by up to 8 orders of magnitude for the two proteins.[25,26]

While there has been a great deal of speculation about the mechanism by which the hydrolysis of the acyl-enzyme intermediates proceeds,[17,26−33] a definitive characterization of the chemistry at an atomic level of detail has yet to be produced. Such a characterization is an essential first step in understanding how the β-lactamase achieves such a dramatic enhancement in hydrolytic activity, despite the sequence conservation in the active site discussed above. Once the mechanism is understood, progress can be made in determining the crucial differentiation between the β-lactamase and PBP. These insights in turn can facilitate both structure-based drug design efforts to develop new antibiotics that are not susceptible to β-lactamase hydrolysis and protein design studies in which the goal is to increase the hydrolytic activity of a PBP up to the level of a β-lactamase with a minimal number of mutations.

In the present paper, we begin by investigating a number of proposed mechanisms for hydrolysis of the acylated enzyme by the β-lactamase and PBP, using ab initio-based mixed quantum mechanics/molecular mechanics (QM/MM) techniques. For the β-lactamase, we present a complete mechanistic analysis which is in good quantitative agreement with experimental data. For the PBP, the mechanisms we have investigated to date yield very slow rates of hydrolysis, in qualitative agreement with experiment. However, none of the obvious pathways for the PBP provide quantitative agreement with measured rate constants. We suggest an alternative mechanism, requiring substantial rearrangement of the enzyme active site, which will be explored further in a subsequent publication. The structural features leading to the dramatic differences between β-lactamase and PBP deacylation rates are elucidated by these analyses at an atomic level of detail.

Our calculations employ very large quantum mechanical active site regions (∼150 QM atoms), and high quality density functional methods along with large basis sets are used to compute the structures and energies of the intermediates and transition states. The expected accuracy of such an approach is substantially greater than previous efforts to model systems of this type,[34−38] as has been extensively demonstrated in our previous work via comparison with experiment for a wide variety of enzymatic reactions (see below).

The paper is organized as follows. In section II, we briefly review our QM and QM/MM methodology and discuss its application to the present problem. Benchmark data from previous QM/MM protein modeling efforts are summarized to provide a picture of what sort of quantitative performance can be expected from the methodology at this point in time. In section III, the physical models for the PBP and β-lactamase are presented, and the various alternatives for the reaction mechanism are enumerated. Section IV presents the results and discussion, providing quantitative calculations of free energy barriers for the various mechanisms, and an atomic level explanation as to the origin of the difference between the hydrolysis rates of the two enzymes. Finally, in the conclusion, we summarize our results and discuss future work.

II. QM and QM/MM Methodology

A. QM Methods. Our core computational method for the QM region in QM/MM calculations is hybrid density functional theory (DFT), specifically the B3LYP functional.[39−41] These methods have been shown to yield excellent results for atomization energies and transition states in a wide range of chemical systems.[42−44] Errors for atomization energies using the G3 database as a test set are on the order of 3 kcal/mol for organic molecules.[45] In the present system, where only one bond is being broken, there will be more cancellation of error than in a typical atomization energy calculation, and we therefore expect that the errors due to the use of DFT are likely to be less than this value, on the order of 1−2 kcal/mol. To obtain the accuracy cited above, it is for some systems necessary to employ large basis sets in the evaluation of energy differences. We have extensively tested a protocol in which geometry optimizations are carried out with smaller, but still quite respectable basis sets (6-31G*), followed by single point calculations using the cc-pVTZ(-f) correlation consistent basis set of Dunning and coworkers.[46] Basis set effects in the present case are quantitatively noticeable, but do not affect our qualitative conclusions concerning the reaction mechanisms.

The Jaguar suite of ab initio quantum chemical programs[47] is used to carry out all QM calculations. Jaguar is particularly efficient for treating large molecules with large basis sets, and is able to handle geometry optimizations and transition state searches for the ∼150 atom QM regions that are investigated in the present paper.[48] Frequency calculations to estimate zero point energies are performed with smaller models and basis sets, as these have a minimal effect on the desired quantities.

B. QM/MM Methods. Over the past several years, we have developed methods for QM/MM calculations based on the use of frozen orbitals as the interface between the QM and MM regions.[49−51] The methodology has been specifically optimized for modeling protein

(24) Sequence homology and alignment was determined using the Vector Alignment Search Tool (VAST), made available by the National Center for Biotechnology Information (NCBI) at the NIH.
(25) Frère, J. M.; Ghuysen, J.-M.; Iwatsubo, M. *Eur. J. Biochem.* **1975**, *57*, 343−351.
(26) Dubus, A.; Ledent, P.; Lamotte-Brasseur, J.; Frère, J. M. *Proteins: Struct., Funct., Genet.* **1996**, *25*, 473−485.
(27) Bulychev, A.; Massova, I.; Miyashita, K.; Mobashery, S. *J. Am. Chem. Soc.* **1997**, *119*, 7619−7625.
(28) Powers, R. A.; Caselli, E.; Focia, P. J.; Prati, F.; Shoichet, B. K. *Biochemistry* **2001**, *40*, 9207−9214.
(29) Oefner, C.; Darcy, A.; Daly, J. J.; Gubernator, K.; Charnas, R. L.; Heinze, I.; Hubschwerlen, C.; Winkler, F. K. *Nature* **1990**, *343*, 284−288.
(30) Dubus, A.; Normark, S.; Kania, M.; Page, M. G. P. *Biochemistry* **1994**, *33*, 8577−8586.
(31) Lobkovsky, E.; Billings, E. M.; Moews, P. C.; Rahil, J.; Pratt, R. F.; Knox, J. R. *Biochemistry* **1994**, *33*, 6762−6772.
(32) Wilkin, J. M.; Jamin, M.; Damblon, C.; Zhao, G. H.; Joris, B.; Duez, C.; Frère, J. M. *Biochem. J.* **1993**, *291*, 537−544.
(33) Bernstein, N. J.; Pratt, R. F. *Biochemistry* **1999**, *38*, 10 499−10 510.
(34) Castillo, R.; Silla, E.; Tunon, I. *J. Am. Chem. Soc.* **2002**, *124*, 1809−1816.
(35) Hata, M.; Fujii, Y.; Ishii, M.; Hoshino, T.; Tsuda, M. *Chem. Pharm. Bull.* **2000**, *48*, 447−453.
(36) Fujii, Y.; Hata, M.; Hoshino, T.; Tsuda, M. *J. Phys. Chem. B* **2002**, *106*, 9687−9695.
(37) Diaz, N.; Suarez, D.; Sordo, T. L.; Merz, K. M. *J. Phys. Chem. B* **2001**, *105*, 11 302−11 313.
(38) Massova, I.; Kollman, P. A. *J. Comput. Chem.* **2002**, *23*, 1559−1576.
(39) Johnson, B. G.; Gill, P. M. W.; Pople, J. A. *J. Chem. Phys.* **1993**, *98*, 5612−5626.
(40) Lee, C. T.; Yang, W. T.; Parr, R. G. *Phys. Rev. B* **1988**, *37*, 785−789.
(41) Becke, A. D. *J. Chem. Phys.* **1993**, *98*, 1372−1377.
(42) Becke, A. D. *J. Chem. Phys.* **1993**, *98*, 5648−5652.
(43) Curtiss, L. A.; Raghavachari, K.; Redfern, P. C.; Pople, J. A. *J. Chem. Phys.* **1997**, *106*, 1063−1079.
(44) Bauschlicher, C. W. *Chem. Phys. Lett.* **1995**, *246*, 40−44.
(45) Curtiss, L. A.; Raghavachari, K.; Redfern, P. C.; Pople, J. A. *J. Chem. Phys.* **2000**, *112*, 7374−7383.
(46) Dunning, T. H. *J. Chem. Phys.* **1989**, *90*, 1007−1023.
(47) Jaguar v4.1 Schrödinger, Inc., Portland, Oregon, 2000.
(48) Friesner, R. A.; Murphy, R. B.; Beachy, M. D.; Ringnalda, M. N.; Pollard, W. T.; Dunietz, B. D.; Cao, Y. X. *J. Phys. Chem. A* **1999**, *103*, 1913−1928.
(49) Philipp, D. M.; Friesner, R. A. *J. Comput. Chem.* **1999**, *20*, 1468−1494.
(50) Murphy, R. B.; Philipp, D. M.; Friesner, R. A. *J. Comput. Chem.* **2000**, *21*, 1442−1457.
(51) Murphy, R. B.; Philipp, D. M.; Friesner, R. A. *Chem. Phys. Lett.* **2000**, *321*, 113−120.

active sites, with parametrization enabling the QM region to be defined via a series of cuts in the backbone and at side chains between the alpha- and beta-carbon. Details of the energy function and analytical gradients, as well as the numerical implementation, are presented in refs 49−51.

The methods are implemented in the QSite program[52] which has been constructed via a tight coupling of Jaguar[47] and the IMPACT protein modeling program of Levy and co-workers.[53] The OPLS-AA protein molecular mechanics force field of Jorgensen and co-workers is used to represent the MM region.[54,55] Capabilities for efficient minimization and transition state optimization have been implemented and extensively tested. A key feature of the methodology is the use of an adiabatic approach to optimization in which the MM region is fully optimized after each QM step, resulting in very large reductions in computational effort as compared to carrying out a QM gradient evaluation at each geometry step (CPU times are in fact a small multiple of those required for an equivalent purely QM calculation).

We have extensively tested the QSite methodology on a wide variety of problems, comparing with both fully QM calculations and, more recently, with experimental data. The following is a brief summary of the tests that have been performed, and the results obtained from them:

(1) Relative energies for multiple conformers of dipeptides incorporating each of the 20 amino acid side chains (including the various relevant protonation states) were determined via accurate fully quantum mechanical calculations, with a total of ∼200 such conformers evaluated in all.[49−51] The average error for the QM/MM relative energies, as compared to the QM calculations, is substantially less than 1 kcal/mol, and comparable to or smaller than the errors obtained on the same test set for the force field itself.

(2) The deprotonation energy for a number of side chains was calculated using QM and QM/MM models.[50,51] The errors in the QM/MM calculations were uniformly less than 2 kcal/mol, and were larger than 1 kcal/mol only when the QM/MM interface was very close to the site of proton removal (less than 5 Å), a situation that would be avoided in most applications.

(3) The binding energy resulting from addition of dioxygen to a ∼60 atom model of the hemerythrin active site (consisting of two iron atoms and 7 side chain analogues ligated to these atoms) was calculated via fully QM calculations and using a series of QM/MM models in which an increasing number of side chain analogues were treated at the QM level.[56] The errors in the QM/MM calculation of the binding affinity were uniformly less than 2 kcal/mol, despite the fact that the QM/MM models were not geometrically reoptimized. Further tests on hemerythrin, using the full QM/MM model incorporating the entire protein and systematically increasing the size of the QM region, yielded errors on the order of 1 kcal/mol when reoptimization of the model for each QM region definition was carried out.

These tests lead to the conclusion that the error induced by the use of QM/MM, as compared to fully QM calculations, is typically less than 1 kcal/mol, a small quantity when compared with the intrinsic accuracy of the DFT calculations (as well as errors induced by incomplete knowledge of the structure, approximately modeled solvation effects, etc.). This conclusion is supported by the comparisons we have made thus far with experimental data on enzymatic systems, obtained without the use of any adjustable parameters:

(1)The free energy of dioxygen binding to hemerythrin was calculated to be 5.2 kcal/mol,[57] in good agreement with the experimental results of 7.3 kcal/mol.[58]

(2)The free energy of activation of methane hydroxylation by methane monooxygenase (MMO) has recently been computed to be 17.8 kcal/mol,[59] whereas the experimental value is 16.5 kcal/mol.[60]

(3)We computed the free energy of activation of the hydroxylation reaction in cytochrome P450cam to be ∼8 kcal/mol.[61] While there is no accurate experimental value available for this quantity, our results predict a very rapid reaction, in qualitative agreement with the experimental inability to trap the precursor intermediate species (compound I),[62] and in distinct contrast to previous work using small QM models which obtained a barrier height of ∼27 kcal/mol.[63]

(4) In addition to these QM/MM calculations, we have performed additional pure QM calculations on a number of reactions in MMO, using a large QM active site model of ∼100 atoms.[64−66] The results of calculations examining the formation of H_{peroxo} and the transformation of H_{peroxo} to the catalytically competent intermediate Q (two reactions for which the interaction of the protein with the relevant reactive region can be essentially encompassed by a QM model) can be compared with experimental data.[67−70] The calculated barrier heights agree with the experimental data to an accuracy of 2−3 kcal/mol, comparable to the comparisons cited above.

The conclusions from the above data are the following: (a) the use of the QM/MM methodology adds little error to what is already present in the QM calculations; (b) there are large contributions of the peripheral MM environment for some reactions; and (c) overall, we can expect the entire protocol−large basis set DFT combined with our QM/MM methodology as implemented in QSite−to yield free energies accurate to within 2−3 kcal/mol, as long as the simplifying approximations that we have employed to compute entropy effects are valid (this approach may have larger errors if the entropy of binding a large, flexible ligand to the protein has to be computed, something that is not an issue in the work presented below). These error bars are sufficient in most cases for qualitative discrimination of mechanisms, and provide a respectable, if not perfect, quantitative picture of the reaction at an atomic level of detail.

A final point that is important to discuss is the treatment of solvation effects. Several of the previous enzymes that we have studied (MMO,[59] cytochrome P450,[50,61] hemerythrin[57]) have active sites that are deeply buried in the protein interior with minimal exposure to bulk water. In these cases, the simple approach of neutralizing ionizable groups on the protein surface (thus implicitly incorporating dielectric screening into the model) appears to work quite well.

The present case is somewhat more complicated. While the ligand and active site tyrosine residue are reasonably well buried in both R61[71]

(52) QSite Schrödinger, Inc., Portland, Oregon, 2000.
(53) Impact v1.7 Schrödinger, Inc., Portland, Oregon, 2000.
(54) Jorgensen, W. L.; Maxwell, D. S.; Tirado-Rives, J. *J. Am. Chem. Soc.* **1996**, *118*, 11 225−11 236.
(55) Kaminski, G. A.; Friesner, R. A.; Tirado-Rives, J.; Jorgensen, W. L. *J. Phys. Chem. B* **2001**, *105*, 6474−6487.
(56) Wirstam, M.; Gherman, B. F.; Guallar, V.; Murphy, R. B.; Friesner, R. A. Manuscript in preparation.
(57) Wirstam, M.; Lippard, S. J.; Friesner, R. A. *J. Am. Chem. Soc.* **2003**, *125*, 3980−3987.
(58) Lloyd, C. R.; Eyring, E. M.; Ellis, W. R. *J. Am. Chem. Soc.* **1995**, *117*, 11 993−11 994.
(59) Gherman, B. F.; Lippard, S. J.; Friesner, R. A. *J. Am. Chem. Soc.*, submitted.
(60) Ambundo, E. A.; Friesner, R. A.; Lippard, S. J. *J. Am. Chem. Soc.* **2002**, *124*, 8770−8771.
(61) Guallar, V.; Baik, M.-H.; Lippard, S. J.; Friesner, R. A. *Proc. Natl. Acad. Sci. U.S.A.* **2003**, *100*, 6998−7002.
(62) Davydov, R.; Makris, T. M.; Kofman, V.; Werst, D. E.; Sligar, S. G.; Hoffman, B. M. *J. Am. Chem. Soc.* **2001**, *123*, 1403−1415.
(63) Ogliaro, F.; Harris, N.; Cohen, S.; Filatov, M.; De Visser, S. P.; Shaik, S. *J. Am. Chem. Soc.* **2000**, *122*, 8977−8989.
(64) Dunietz, B. D.; Beachy, M. D.; Cao, Y. X.; Whittington, D. A.; Lippard, S. J.; Friesner, R. A. *J. Am. Chem. Soc.* **2000**, *122*, 2828−2839.
(65) Gherman, B. F.; Dunietz, B. D.; Whittington, D. A.; Lippard, S. J.; Friesner, R. A. *J. Am. Chem. Soc.* **2001**, *123*, 3836−3837.
(66) Gherman, B. F.; Baik, M.-H.; Lippard, S. J.; Friesner, R. A. *J. Am. Chem. Soc.*, **2004**, *126*, 2978−2990.
(67) Brazeau, B. J.; Lipscomb, J. D. *Biochemistry* **2000**, *39*, 13 503−13 515.
(68) Liu, K. E.; Wang, D. L.; Huynh, B. H.; Edmondson, D. E.; Salifoglou, A.; Lippard, S. J. *J. Am. Chem. Soc.* **1994**, *116*, 7465−7466.
(69) Liu, K. E.; Valentine, A. M.; Wang, D. L.; Huynh, B. H.; Edmondson, D. E.; Salifoglou, A.; Lippard, S. J. *J. Am. Chem. Soc.* **1995**, *117*, 10 174−10 185.
(70) Valentine, A. M.; Stahl, S. S.; Lippard, S. J. *J. Am. Chem. Soc.* **1999**, *121*, 3876−3887.
(71) Kuzin, A. P.; Liu, H. S.; Kelly, J. A.; Knox, J. R. *Biochemistry* **1995**, *34*, 9532−9540.

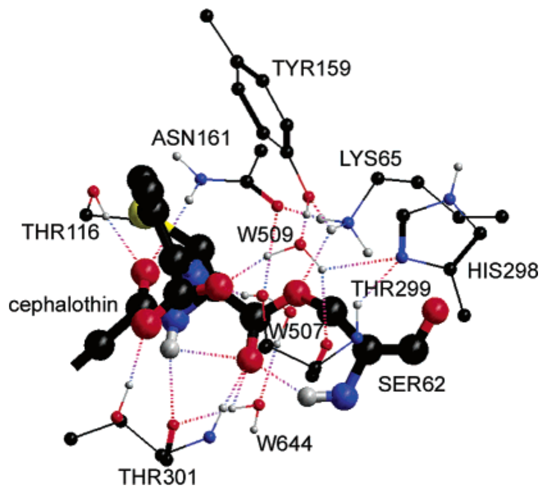

Figure 1. R61-PBP active site, with the cephalothin-Ser62 covalent linkage highlighted. Dashed lines indicate hydrogen bonds. Color coding: C-black, N-blue, O-red, H-gray, S-yellow.

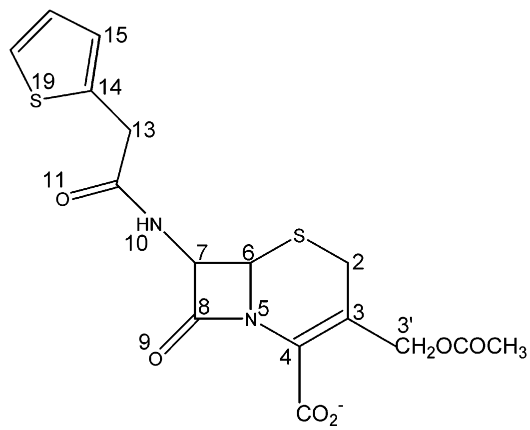

Figure 2. Structure of the β-lactam antibiotic cephalothin.

and P99,[31] other groups such as Lys315, Glu272, and Arg148 in the P99 β-lactamase are partially exposed. One possible approach is to use a continuum solvation model. However, these groups are surrounded by ordered waters (which can be seen in the crystal structures[31,71]), and it is unclear whether a continuum solvent model provides an accurate description of such waters in a confined space. Therefore, we have chosen to treat these waters explicitly at a molecular mechanics level, with the exception of the catalytic waters W509/W402 in R61/P99, which are included in the QM regions. Given that the waters are visible in the crystal structures, our assumption is that extensive sampling over their positions is unnecessary, making an explicit treatment tractable. Furthermore, the good agreement that we obtain with experimental rate constants (vide infra) suggests that this treatment is a reasonable one. In future work, we intend to supplement the explicit ordered waters with a continuum treatment of the unstructured bulk water in the outer shells. For the present system, the retention of ordered crystal waters, coupled with neutralization of ionizable surface groups distant from the active site, appears to lead to relatively small errors, based on the results discussed below.

III. Physical System and Computational Models

Our starting point is a cocrystallized structure of the antibiotic cephalothin with the penicillin binding protein *Streptomyces* sp. R61 DD-peptidase.[71] The active site of this structure is depicted in Figure 1. Key features of the structure have been noted previously.[71] The ligand is acylated to Ser62 at its C8 carbonyl position (Figure 2), involving the usual ester linkage of this carbon with the O-γ of the serine. The carbonyl oxygen on what was formerly the lactam ring, O9 (i.e., the carbonyl oxygen attached to C8), resides in the oxyanion hole, where it hydrogen bonds with backbone amide −NH groups from residues Ser62 and Thr301. Other important hydrogen bonds, which anchor the ligand in place, are indicated in Figure 1.

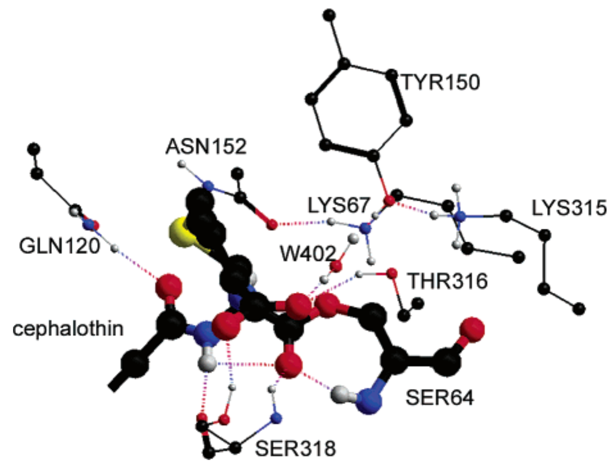

Figure 3. P99 β-lactamase active site, with the cephalothin-Ser64 covalent linkage highlighted. Dashed lines indicate hydrogen bonds. Color coding: C-black, N-blue, O-red, H-gray, S-yellow.

To compare the hydrolysis of cephalothin by the P99 cephalosporinase with this same reaction in the R61-PBP, it was necessary to construct a suitable complex by docking the ligand into the β-lactamase. Assembly of the protein−ligand complex was facilitated by examination of the PBP-cephalothin acyl-enzyme intermediate discussed above[71] and of a transition state analogue phosphonate derivative of the *Enterobacter cloacae* P99 cephalosporinase.[31] The active site resulting from the docking of cephalothin into P99, after molecular mechanics and QM/MM optimization, is presented in Figure 3. Initial positioning of the ligand in the active site was accomplished primarily by enforcing key covalent and hydrogen bonds between the protein and ligand based on the structures discussed above (e.g., placing of the carbonyl oxygen O9 of the ligand in the oxyanion hole, in this case defined by the −NH groups of Ser64 and Ser318). It should be mentioned that, once the ligand was docked as described, all calculations were carried out with the resulting structure. That is, there was no attempt to reposition the ligand so as to, for example, obtain a lower activation barrier.

A number of proposals have been made in the literature with regard to the mechanism of the hydrolysis reaction for the PBP and β-lactamase,[17] the main focus of the present paper. All involve an attack by W509 in R61 (Figure 1) or the analogous W402 in P99 (Figure 3) on the C8 ligand carbon acylated to serine, leading to formation of a tetrahedral intermediate, followed by decay of that intermediate to release product. The key issue is the means by which the water molecules are activated. Without such activation, the barrier to forming the tetrahedral intermediate is prohibitively high. To carry out this activation, a general base is required to accept a proton from the water, and it is in the identity of the general base that the various proposals differ.

The first alternative that we consider is that the lactam nitrogen atom, N5, in the cephalothin ligand could serve as the general base.[27,28] We investigated this proposal in some detail, using both QM and QM/MM methods, but obtained barrier heights in the range of 63−74 kcal/mol in R61 and 44−49 kcal/mol in P99, considerably higher than both experimental observations and computational results for the alternative pathways (vide infra). This mechanism is energetically unfavorable due to the lactam nitrogen being a weak general base. The volume of space between N5 and the serine/ligand ester group is also limited, making approach of the catalytic water molecule into this area a high energy process. We therefore rejected this mechanism as inconsistent with both theory and experiment, and will not consider it in the remainder of this paper. A second possibility is that Lys65/67 in R61/P99 serves as

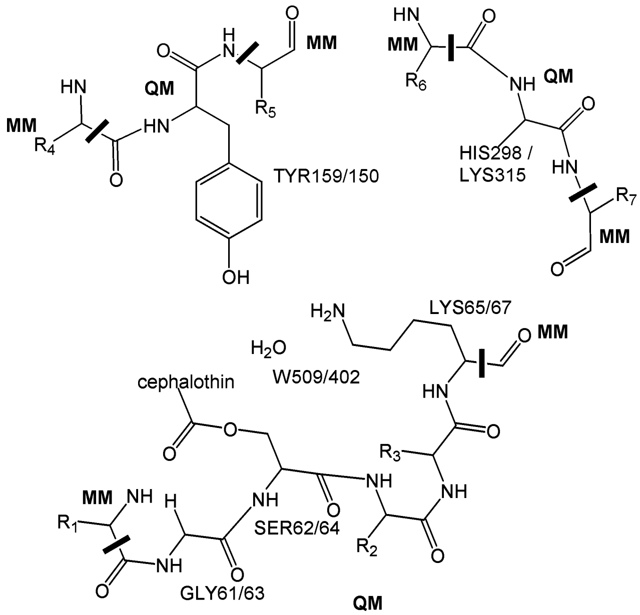

Figure 4. Model used for QM/MM calculations.

the general base.[30] Its ability to do so depends on its protonation state (only a deprotonated lysine could act as a proton acceptor) and geometry (the lysine would initially have to form a hydrogen bond with the water molecule). As will be discussed below, the Lys65/67 mechanism is an important alternative only for the R61 system. For P99, the Tyr150 model, discussed below, is clearly qualitatively superior with regard to lowering the barrier to formation of the tetrahedral intermediate (although in mutant P99 enzymes in which Tyr150 is changed to a different amino acid, the Lys67 mechanism may become relevant). Therefore, we discuss the Lys65 mechanism only for R61 in what follows.

The third, and final, proposal is that Tyr159/150 in R61/P99 acts as the general base, either in a deprotonated form or in a state exhibiting a substantial partial negative charge stabilized by neighboring groups in the protein.[26,29,31−33] In order for a tyrosine to function effectively as a general base, a specialized protein environment is required. The key residues in this regard are Lys65/67 in R61/P99 and, in the β-lactamase, Lys315. Interactions of the tyrosine with the ligand, which is in close proximity to the tyrosine oxygen (particularly for R61), also have an influence on the energetics of the tyrosine in its various possible protonation states. A detailed analysis of the tyrosine mechanism for both the R61 and P99 systems is presented below.

To investigate these mechanistic proposals with an accurate computational model, we have constructed the QM regions of our QM/MM model as depicted in Figure 4. Included in the QM region for R61/P99 are the ligand, Gly61/63, Ser62/64, Tyr159/150, W509/402, and the side chains from Lys65/67 and His298/Lys315. The total number of atoms in the QM region is ~150, representing the largest QM/MM calculation that we have attempted to date.

A key structural aspect of the physical model is the assignment of protonation states and the positions of hydrogen atoms, information that is not directly available from the X-ray crystal structures. As was mentioned above, we neutralized ionizable groups on the protein surface that are far from the active site in order to mimic the effect of the high dielectric solvent. In the active site itself, the protonation states and hydrogen positions are central to the question of the catalytic mechanism, as will be discussed in more detail below. Protons can be placed in a number of different locations to form different hydrogen bonding patterns. We investigate a number of such patterns in what follows. In this analysis, the R61 and P99 structures must be considered individually. In each case, our focus is on the Tyr159/150 hydroxyl group in R61/P99 and its surrounding residues, as it is the ability of this group to serve as a general base in the reaction which is the key to the catalytic activity (at least as is available from this mechanism) of the two proteins.

We consider the P99 structure first. If Tyr150 is to act as a general base and activate W402, then a hydrogen from that water must be hydrogen bonded to the hydroxyl oxygen in the acyl-enzyme intermediate. This oxygen (whether deprotonated or simply possessing a large partial negative charge) will induce a substantially larger positive charge on the hydrogen of the water, thus in turn leading to an increased negative charge on the water oxygen, which allows the nucleophilic attack on C8 of the ligand to proceed with a relatively low barrier (facilitated, of course, by positioning of the carbonyl group of the ligand in the oxyanion hole, onto which the negative charge from the attacking oxygen can be delocalized).

If this water is indeed hydrogen bonded to the hydroxyl oxygen, then, unless the hydroxyl proton is removed, the oxygen can accept only one additional hydrogen bond from a neighboring hydrogen bond donor. On the basis of the distances extracted from the crystal structure, the terminal nitrogens of both Lys67 and Lys315 are within hydrogen bonding distance of the oxygen. This leads to two different types of structures, which can be enumerated as follows:

(a) The hydroxyl hydrogen remains on the tyrosine, and forms a hydrogen bond with either Lys67 or Lys315. If this occurs, the lysine in question must be itself uncharged. Otherwise, it would not be able to accept the hydrogen bond from the donor hydrogen. The other lysine is assumed to be protonated.

(b) The tyrosine can be deprotonated, in which case both lysine residues must be charged. There is no other group within the relevant distance capable of hydrogen bonding to the nitrogen on either lysine residue. In addition, it is inconceivable, given the intrinsic basicity of the ammonium group, that the uncharged form could be lower in energy than the charged form without a hydrogen bond to that group.

This analysis leads to three possible structures, all of which are potential candidates for a mechanism in which Tyr150 acts as the general base activating W402:

(1) Lys67 protonated, Lys315 neutral, Tyr150 protonated with proton hydrogen bonded to Lys315.

(2) Lys315 protonated, Lys67 neutral, Tyr150 protonated with proton hydrogen bonded to Lys67.

(3) Lys315 and Lys67 protonated, Tyr150 deprotonated.

The three structures are depicted in detail in Figure 5. Note that the net charge of the entire moiety is +1 in all three cases, and that the differences between them are in essence 1 Å shifts of a proton. The conclusion that it is impossible to protonate both lysine groups without deprotonating the tyrosine is also important. Previous papers have simply assumed that both lysine groups have a positive charge, and then proceeded to speculate about the protonation state of the tyrosine.[72,73] The above analysis demonstrates that the protonation states are coupled, and provides an exhaustive enumeration of the combinations that have to be considered. As the net charge of the closely grouped structural moiety is independent of the details of the proton locations, a full scale pK_a calculation is unnecessary. Instead, what is required is quantum chemical evaluation of the relative energies of the various alternatives, which is discussed in the Results section. Other groups in the active site can be considered to be decoupled from this cluster of residues, and can be analyzed independently.

Of the remaining ionizable residues in the protein, the only one sufficiently close to the active site to have a material effect on the activation free energy is Glu272. This residue is relatively solvent exposed and interacts with Lys315 via a bridging water molecule. It also forms a salt bridge interaction with Arg148. In this environment, the carboxylate almost certainly is in its normal, negatively charged,

(72) Fenollar-Ferrer, C.; Frau, J.; Vilanova, B.; Donoso, J.; Munoz, F. *Theochem-J. Mol. Struct.* **2002**, *578*, 19−28.
(73) Fenollar-Ferrer, C.; Frau, J.; Donoso, F.; Munoz, F. *Proteins: Struct., Funct., Genet.* **2003**, *51*, 442−452.

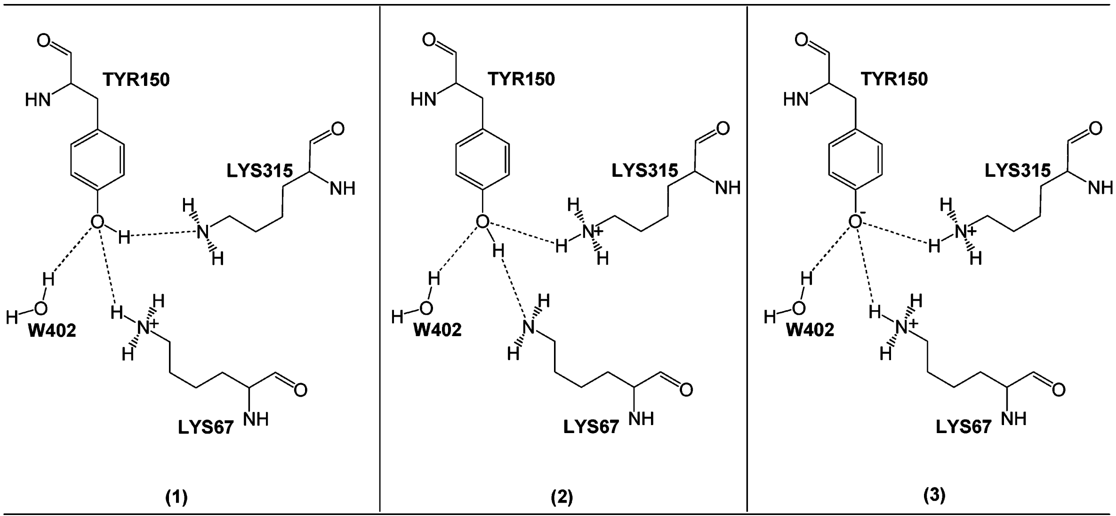

Figure 5. Three possible protonation/hydrogen bond configurations for the acyl-enzyme intermediate in P99. Dashed lines indicate hydrogen bonds.

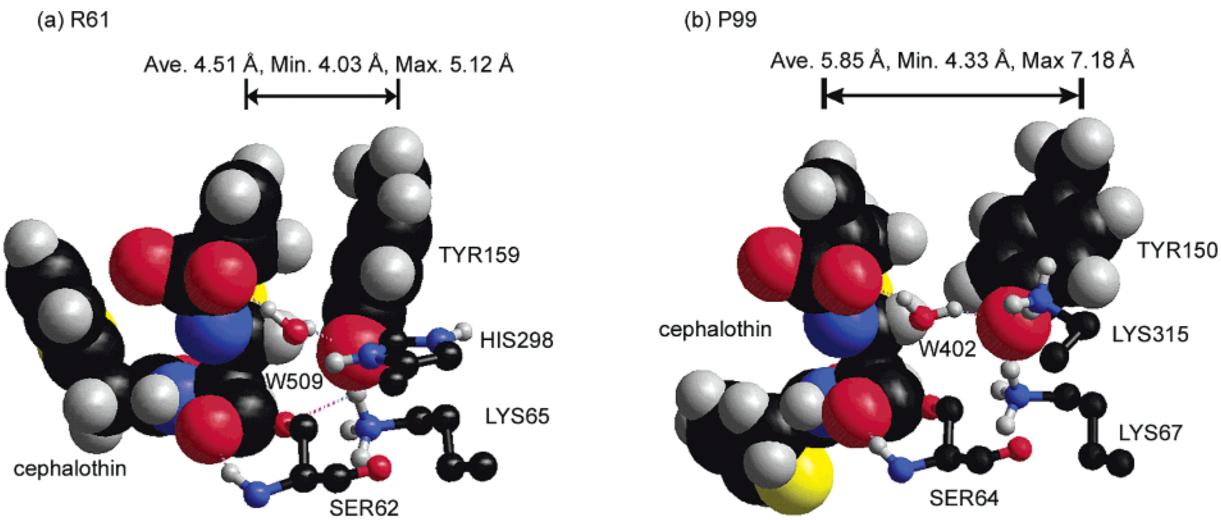

Figure 6. Comparison of the positioning of cephalothin in relation to Tyr159/150 in R61/P99 (shown here in the acyl-enzyme intermediates where tyrosine is deprotonated). Tyr159/150 and cephalothin are shown with space-filling models. Distances are measured between the tyrosine phenyl ring and the cephalothin dihydrothiazine ring. Dashed lines indicate hydrogen bonds. Color coding: C-black, N-blue, O-red, H-gray, S-yellow.

deprotonated state, and we model it accordingly. We also model Arg148 in its protonated state, as otherwise the charge balance of the salt bridge would be incorrectly represented. Crystallographic water molecules hydrogen bonded to the carboxylate and guanidinium groups are included in the calculations (as are other crystallographic waters, all at an MM level), and these provide the appropriate dielectric screening of the carboxylate moiety.

Finally, the carboxylate group in the ligand clearly forms multiple hydrogen bonds to donor groups on Thr316, Ser318, Arg346, W402, and W515, and hence must be in its ionized form. It is also the case that the negative charge on this moiety balances the net +1 charge on the Tyr150-Lys67-Lys315 trio, thus yielding approximate electrical neutrality in the buried region of the active site. Other ionizable groups (excluding those that form a salt bridge, such as Glu272/Arg148) are sufficiently distant from the active site that they can safely be neutralized.

We next turn to an analysis of the active site structure of the R61 acyl-enzyme intermediate. We consider here the hydrogen bond network involving Tyr159, Lys65, W509, and the ester oxygen on the ligand. The remaining interactions of the ligand with the protein are similar to those discussed above for P99. As in the case of P99, there is a water molecule, W509 (which must be activated in order to catalyze the hydrolysis reaction), within hydrogen bonding distance of the phenol oxygen of Tyr159. Lys65 is also within hydrogen bonding distance of Tyr159, in a position analogous to Lys67 in the P99 structure. However, the residue in an equivalent structural position to Lys315, His298, is too distant from the Tyr159 oxygen to form a hydrogen bond of any sort (the closest approach of a His298 side chain nitrogen to the Tyr159 oxygen is 4.6 Å). One reason that His298 cannot form a hydrogen bond to Tyr159 is that its side chain is shorter than that of a lysine, and it cannot reach the relevant target. A second (and ultimately controlling) reason, however, is that further access to the Tyr159 oxygen is blocked by the ligand, due to a different positioning of cephalothin in the active site cavity of R61, which is somewhat tighter than that of P99 (Figure 6). In fact, the ester oxygen originating from Ser62 (and transformed into an ester as a result of the acylation reaction) is observed to be within 3.1 Å of the hydroxyl oxygen of Tyr159, implying that the hydroxyl hydrogen must be interposed between the hydroxyl oxygen and the Ser62 ester oxygen.

In ref 71, the interaction between the Ser62 ester oxygen and Tyr159 is interpreted as forming a strong hydrogen bond. Our assessment is, however, that this hydrogen bond is in fact extremely weak, certainly much weaker than that formed between Tyr150 and the ammonium group of Lys315 in P99. In previous work, we have shown that ester

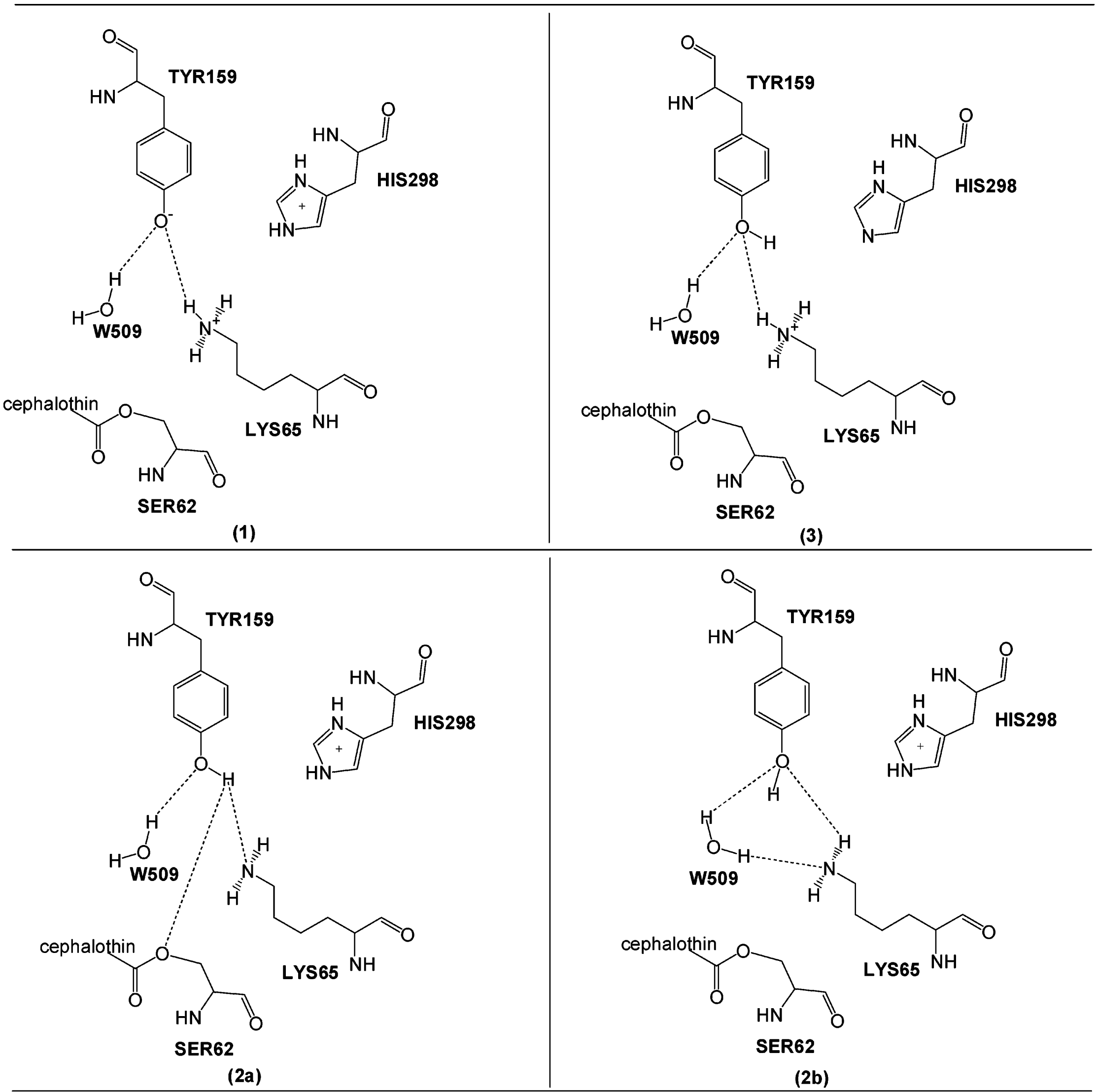

Figure 7. Four possible protonation/hydrogen bond configurations for the acyl-enzyme intermediate in R61. Dashed lines indicate hydrogen bonds.

oxygens are particularly poor hydrogen bond acceptors.[74] For example, the hydrogen bonding energy of a water molecule to methyl formate in the gas phase, computed via reasonably accurate quantum chemical methods, is 3.4 kcal/mol as compared to that for water binding to methanol which using the same methods is 4.9 kcal/mol. Furthermore, quantum chemical geometry optimization of the R61 active site shows that the hydroxyl hydrogen atom is poorly positioned to form a hydrogen bond with the Ser62 ester oxygen (Figure S1). Thus, the positioning of the cephalothin ligand prevents formation of a second strong hydrogen bond (i.e., in addition to Lys65) with a partner capable of accepting the hydroxyl hydrogen, even if one were to be made available (e.g., by mutating His298 to a lysine).

As in the case of P99, there are a number of different possible protonation states for R61. The principle difference is that, unlike Lys315, it is clearly not possible to protonate the ester oxygen of Ser62, which is far too weak a base to accept a proton. Again, the carboxylate group in the ligand forms multiple hydrogen bonds to donor groups on Thr299, Thr301, and W509, and hence must be in its ionized form. His298, located on the periphery of the active site, can be protonated or deprotonated, although its lack of direct interactions with other active site residues makes it very unlikely that its protonation state will materially affect the hydrolysis reaction. Moreover, unlike Glu272 in P99, there is no hydrogen bond network connecting His298 with the Tyr159 side chain oxygen. The protonation state of His298 was set therefore based upon the net charge of the Tyr159/Lys65 couple in order to yield overall electrical neutrality in the buried active site. Hence, the important questions are the protonation states and hydrogen atom positions (i.e., hydrogen bond patterns) of Lys65 and Tyr159. As in the case of the P99 active site, there are a number of possibilities (Figure 7):

(1) Tyr159 is deprotonated and Lys65 is protonated (with His298 protonated), thus forming a neutral salt bridge. W509 also hydrogen bonds to Tyr159. This is the configuration that is consistent with Tyr159 acting as a general base (analogously to the P99 models discussed above).

(2) Tyr159 is protonated and Lys65 is not protonated (with His298 protonated), i.e., these two moieties are both electrically neutral. W509 donates a hydrogen bond to the side chain oxygen of Tyr159. There are then two possible completions of the hydrogen bonding pattern:

(a) The Tyr159 hydroxyl hydrogen forms a strong hydrogen bond with the terminal nitrogen of Lys65 and a weak hydrogen bond with the ester oxygen of Ser62. This configuration is consistent with the protonated form of Tyr159 acting as a general base, with the transfer of a proton from Tyr159 to Lys65 occurring in concert with transfer of the water hydrogen to the tyrosine (which retains a hydrogen bond with the then activated water).

(74) Marten, B.; Kim, K.; Cortis, C.; Friesner, R. A.; Murphy, R. B.; Ringnalda, M. N.; Sitkoff, D.; Honig, B. *J. Phys. Chem.* **1996**, *100*, 11 775−11 788.

Table 1. Protonation/Hydrogen Bond Configurations for the P99 Acyl-Enzyme Intermediate

configuration	Tyr150	Lys67	Lys315	general base	relative energy (kcal/mol)
1	protonated	protonated	deprotonated	not catalytically competent	+7.7
2	protonated	deprotonated	protonated	Tyr150/Lys67	+1.8
3	deprotonated	protonated	protonated	Tyr150	0.0

(b) The Tyr159 hydroxyl oxygen forms a hydrogen bond with one of the H_ζ at the Lys65 terminus. The terminal nitrogen of Lys65 accepts a hydrogen bond from the W509 hydrogen atom not already engaged in hydrogen bonding to Tyr159. In this case, the Tyr159 hydroxyl hydrogen remains interposed between the hydroxyl and Ser62 ester oxygens, although Tyr159 has shifted position sufficiently so that there is no longer a Tyr159-ester hydrogen bond. However, as discussed above, this was a weak hydrogen bond in any case, so arguably the resulting structure is not grossly unfavorable. This configuration is consistent with Lys65 acting as the general base.

(3) Tyr159 protonated and Lys65 protonated (with His298 deprotonated). Although Lys65 is buried in the protein with no solvent exposure, the same can be said for His298, making this case equally as realistic as case (2). P99 contrasts with this situation, where Lys67 is buried but Lys315 is considerably more solvent exposed. It should be noted though that since both Tyr159 and Lys65 are protonated, this protonation state cannot be catalytically competent.

IV. Results

A. Overview. We first analyze the hydrolysis reaction for the R61 and P99 systems individually. QM/MM calculations are used to determine the free energy barriers for formation of the tetrahedral intermediate. The results of these calculations are shown to be in good qualitative (and, in the case of P99, quantitative) agreement with experimental kinetic data for the deacylation rates of the acyl-enzyme intermediates for R61 and P99 with cephalothin,[25,26] thus providing confidence that the calculations, despite a number of approximations, yield a sound basis for understanding the key features differentiating the β-lactamase and PBP with regard to deacylation rates.

We then extract a qualitative picture of the underlying chemistry, and investigate whether this picture is supported by other data for PBPs and β-lactamases, for example the effects of mutations upon hydrolysis rate constants.[26,30,75−81] This discussion is preliminary in nature, but provides significant evidence that our conclusions are consistent with this broader range of experimental observations. Given the complexity of the system and the challenging nature of the calculations (these are the largest, and most spatially dispersed, QM/MM calculations we have attempted to date, and the active site has substantial solvent exposure in some relevant locations), the ability to explain a series of otherwise puzzling results is an essential component of our belief that we have made significant progress in understanding the efficacy of class C β-lactamases toward deacylation as compared to PBPs.

B. QM/MM Calculations on P99. The initial step is to determine which of the three protonation states for the acyl intermediate has the lowest energy. We have carried out QM/MM geometry optimizations of the three protonation states discussed above in Section III, using the QM/MM model specified therein. The relative energies of the three structures are listed in Table 1; active site geometries are depicted in the Supporting Information (Figure S2).

It is clear on simply physical grounds that neutralization of Lys315 is unacceptable. This lysine has substantial solvent exposure, as well as a relatively close interaction (via a bridging water) with the negatively charged carboxylate on Glu272. This conclusion is supported by the quantitative QM/MM calculations in Table 1 which indicate that the state with Lys315 neutralized is 5.9 kcal/mol higher than any alternative. The question of whether the proton originating on the Tyr150 hydroxyl resides closer to the tyrosine oxygen or the Lys67 nitrogen (the remaining two choices) is more subtle. Here, quantitative QM/MM calculations are required to discriminate which of these states is lowest in energy, and the results, indicating that Tyr150 and Lys67 form a salt bridge (by a margin of 1.8 kcal/mol) are decisive but far from obvious. Indeed, this energy difference is likely within the margin of error of the DFT methodology. Note that, given the solvent exposure of Lys315, the buried Lys67 residue must either be neutral or part of a salt bridge.

The next step is to determine the lowest energy transition state. We investigate transition states arising from the two competitive structures (Tyr150 formally charged, i.e., case #3 in Table 1, or neutral, i.e., case #2 in Table 1) presented above. The mechanism stemming from case #2 involves the neutral form of Tyr150 acting as the general base with concerted transfer of a proton from Tyr150 to Lys67, and it is this mechanism which has the lowest energy transition state (Figure 8). At first, this result is counterintuitive. It would be expected that the activation energy would be less for the mechanism involving deprotonated Tyr150 as the general base. Not only does this latter mechanism commence directly from the P99 acyl-enzyme ground state, but it is also in the deprotonated Tyr150 structure that the negative charge on the tyrosine oxygen is largest. However, computations with the large basis set clearly indicate a stabilization of charge separation, leading to a relative increase in the activation barrier for the deprotonated Tyr150 mechanism (during which charge separation decreases as the phenolate attracts the proton from W402) and a corresponding decrease for the Lys67/Tyr150 concerted mechanism (during which charge separation increases as the proton is transferred from Tyr150 to Lys67). Figure 9 presents the optimized transition state structures. In the concerted Lys67/Tyr150 transition state, the hydroxyl proton occupies a position in which it is not formally bonded to the tyrosine oxygen or the lysine nitrogen. The optimal calculated barrier when zero point effects are included, 14.3 kcal/mol, is in excellent agreement with the experimental value of 14.3 kcal/mol (the precision of agreement

(75) Monnaie, D.; Dubus, A.; Cooke, D.; Marchand-Brynaert, J.; Normark, S.; Frère, J. M. *Biochemistry* **1994**, *33*, 5193−5201.
(76) Hadonou, A. M.; Jamin, M.; Adam, M.; Joris, B.; Dusart, J.; Ghuysen, J.-M.; Frère, J. M. *Biochem. J.* **1992**, *282*, 495−500.
(77) Monnaie, D.; Dubus, A.; Frère, J. M. *Biochem. J.* **1994**, *302*, 1−4.
(78) Wilkin, J. M.; Dubus, A.; Joris, B.; Frère, J. M. *Biochem. J.* **1994**, *301*, 477−483.
(79) Dubus, A.; Wilkin, J. M.; Raquet, X.; Normark, S.; Frère, J. M. *Biochem. J.* **1994**, *301*, 485−494.
(80) Trépanier, S.; Knox, J. R.; Clairoux, N.; Sanschagrin, F.; Levesque, R. C.; Huletsky, A. *Antimicrob. Agents Chemother.* **1999**, *43*, 543−548.
(81) Bourguignon-Bellefroid, C.; Wilkin, J. M.; Joris, B.; Aplin, R. T.; Houssier, C.; Prendergast, F. G.; Vanbeeumen, J.; Ghuysen, J.-M.; Frère, J. M. *Biochem. J.* **1992**, *282*, 361−367.

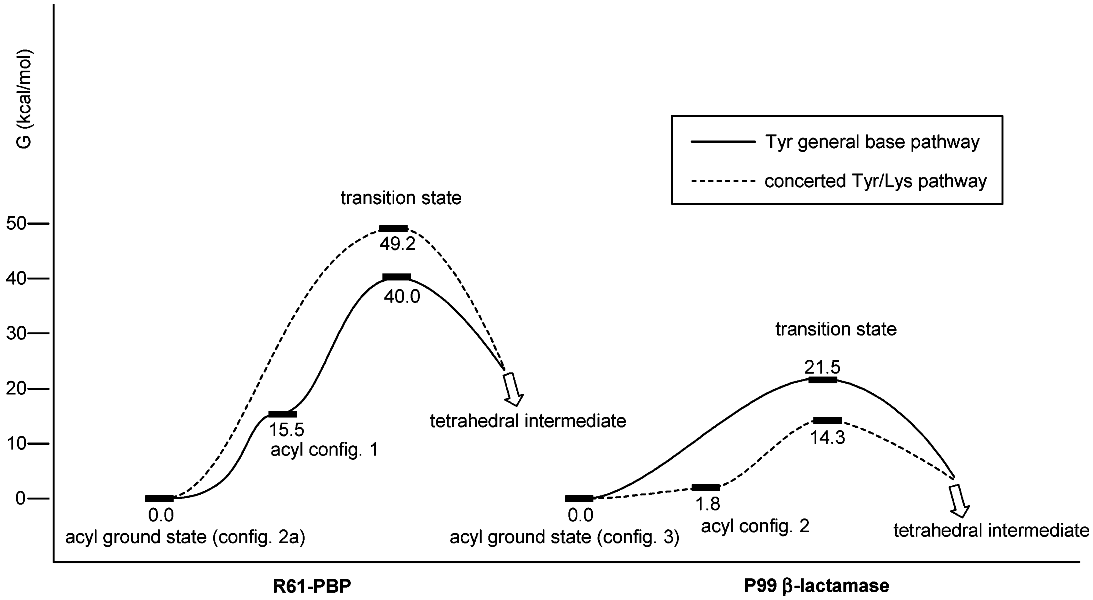

Figure 8. Schematic reaction profile for the deacylation reactions in R61 and P99.

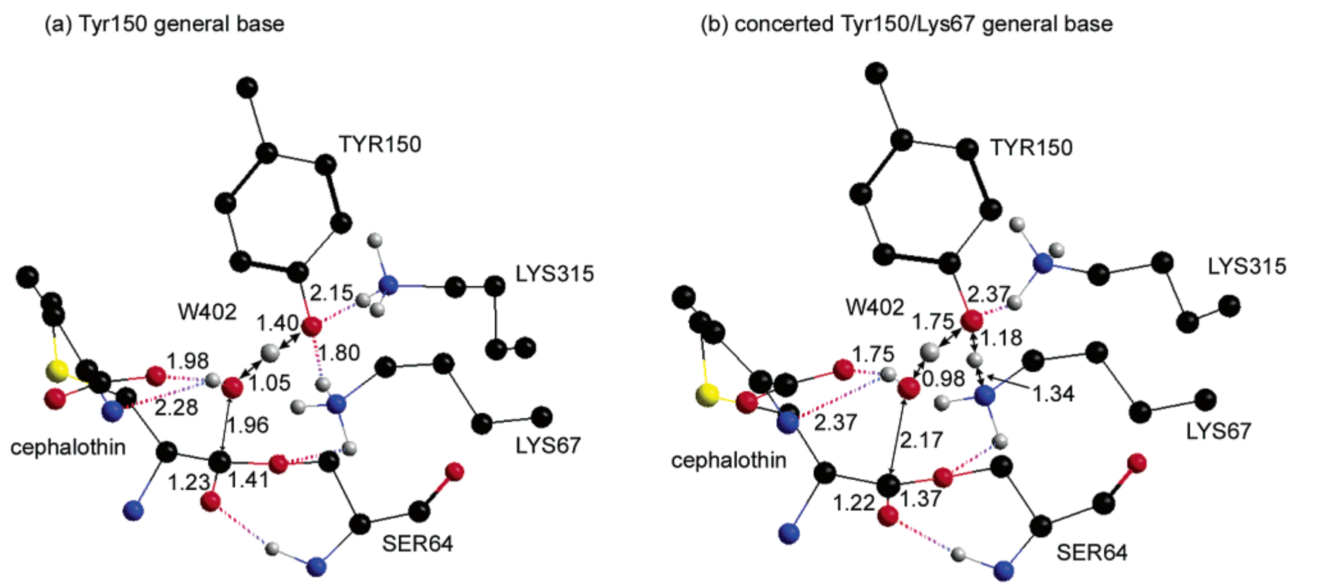

Figure 9. Active site geometries for the QM/MM-optimized transition state structures for P99. Dashed lines indicate hydrogen bonds. Single numbers indicate distances (Å). Color coding: C-black, N-blue, O-red, H-gray, S-yellow.

is undoubtedly fortuitous, given the intrinsic accuracy of the B3LYP functional among other possible sources of error).

C. QM/MM Calculations on R61. For R61, three of the four protonation/hydrogen bond configurations (1, 2a, and 3 above) can be readily produced from the 1CEG PDB crystal structure.[71] However, case 2b is more challenging, because the Lys65 N_ζ is, in the crystal structure, 3.78 Å away from the oxygen of W509. To construct the hydrogen bonding geometry corresponding to 2b, it is necessary to move the lysine from its crystallographic position. Initial attempts to manually position Lys65 in the appropriate location were not successful. The problem is difficult because it must be formulated in a minimum of 12 dimensions. The position of W509, as well as the lysine, can be adjusted to produce an appropriate structure, and other residues may subsequently have to be shifted to accommodate whatever geometry is generated by Lys65 and the water. We have concluded that a more automated approach is necessary, involving the use of an exhaustive side chain prediction algorithm,[82,83] and intend to pursue this in a subsequent publication. Hence, in what follows, quantitative results are presented only for Tyr159-based mechanisms.

From the results of Table 2, the ground state of the system is the structure derived from hydrogen bond pattern 2a, i.e., Tyr159 protonated and Lys65 deprotonated (with a hydrogen bond between the tyrosine and lysine) with His298 protonated. Notably, the structure with both Tyr159 and Lys65 protonated with His298 deprotonated (pattern 3) is only marginally higher in energy. The 15.5 kcal/mol energy difference between the salt bridge and hydrogen bond pattern 2a can be attributed in great part to the lack of suitable additional hydrogen bonding partners for the now negative oxygen on Tyr159. The only such hydrogen

(82) Jacobson, M. P.; Kaminski, G. A.; Friesner, R. A.; Rapp, C. S. *J. Phys. Chem. B* **2002**, *106*, 11 673−11 680.
(83) Andrec, M.; Harano, Y.; Jacobson, M. P.; Friesner, R. A.; Levy, R. M. *J. Struct. Funct. Genomics* **2002**, *2*, 103−111.

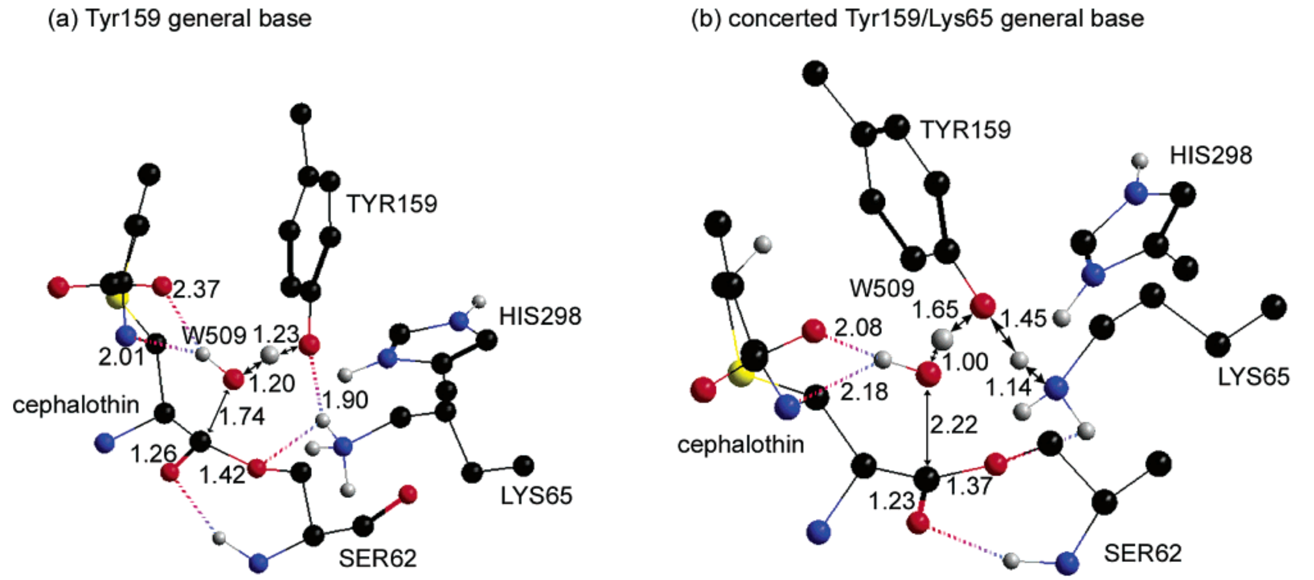

Figure 10. Active site geometries for the QM/MM-optimized transition state structures for R61. Dashed lines indicate hydrogen bonds. Single numbers indicate distances (Å). Color coding: C-black, N-blue, O-red, H-gray, S-yellow.

Table 2. Protonation/Hydrogen Bond Configurations for the R61 Acyl-Enzyme Intermediate

configuration	Tyr159	Lys65	His298	general base	relative energy (kcal/mol)
1	deprotonated	protonated	protonated	Tyr159	+15.5
2a	protonated	deprotonated	protonated	Tyr159/Lys65	0.0
2b	protonated	deprotonated	protonated	Lys65	n/a
3	protonated	protonated	deprotonated	not catalytically competent	+0.5

bond partner (in addition to the protonated Lys65 component of the salt bridge) is the hydrogen from W509. A charged species requires at a minimum a full complement (typically three) of first shell hydrogen bonds (which are worth 10−15 kcal/mol each, 2−3 times more than the hydrogen bonds between two neutral species, even if the partner is neutral) in order to favor its generation. In the present case, the ester oxygen from Ser62 occupies the position that ordinarily would contain a hydrogen bond partner. This is actually worse than, for example, a hydrophobic group because the ester oxygen itself possesses a negative partial charge. In contrast, the P99 enzyme has the positively charged Lys315 in the fourth first shell coordination position, providing the best possible stabilization of a negative charge on the tyrosine oxygen in that system. The deficient access to a second water shell renders salt bridge formation problematic even in P99; in R61, however, the problem is qualitatively more severe.

We next calculate transition states (Figure 10) that can be generated from each of the ground-state structures discussed above. The results of these calculations are shown in Figure 8. The two mechanisms in which Tyr159 serves as the general base both yield free energy barriers that are ∼13−22 kcal/mol too large as compared to experiment, which provides a value of ∼27 kcal/mol.[25] This is well beyond the range of errors expected from either the DFT calculations, errors in the QM/MM model, or issues associated with constructing the models. We conclude that, in R61, Tyr159 cannot be acting as the general base. This is physically unsurprising given the arguments made above concerning the environment of the tyrosine oxygen, which is unsuitable for stabilization of negative charge due to the positioning of the ester oxygen in the first coordination shell as opposed to a group capable of hydrogen bond donation.

In contrast, the mechanism in which Lys65 acts as the general base appears to be a plausible one, provided that it can be correctly positioned geometrically; quantitative assessment of this proposal awaits explicit calculations. Lys65 is unlikely to be as good a general base as is Tyr150 in P99. It lacks the optimized electrostatic environment of the latter (no doubt generated by intense evolutionary pressure). However, the intrinsic basicity of the lysine side chain should enable this residue to act with some effectiveness in a normal hydrogen bonding environment. Of course, the burial of Lys65 in the protein is a critical feature of the mechanism. Without this, the ammonium group would be protonated and hence incapable of acting as a general base under any circumstance. The burial of both Lys65 in R61 and Lys67 in P99 is mandated by the overall protein structure, and this is clearly a key feature of both enzymes. Failure to recognize the consequences of this burial (in many cases, the lysine has simply been assumed to be protonated without any discussion or calculation) has led to confusion in previous efforts to analyze the R61 and P99 active sites.[72,73]

D. Discussion. The hydrolysis reaction we have investigated in this paper would have a much higher activation barrier in free solution than in either of the enzymes considered here. The reaction is feasible at all only because of features common to both active sites, such as stabilization of the tetrahedral intermediate by the oxyanion hole. The fact that quantitative agreement with experiment was obtained for P99, without the use of any adjustable parameters or ad hoc assumptions, suggests that the DFT and QM/MM methodology are capable of properly

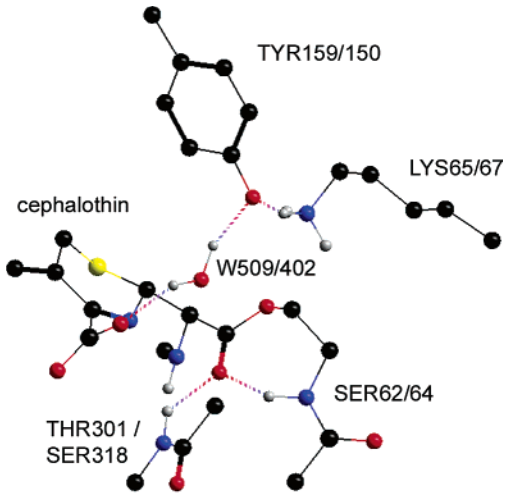

Figure 11. QM model of the R61/P99 active site (acyl-enzyme intermediate form shown). Dashed lines indicate hydrogen bonds. Color coding: C-black, N-blue, O-red, H-gray, S-yellow.

accounting for the electrostatic and quantum mechanical effects driving the catalysis.

The mechanisms providing the extraordinarily low barrier in the P99 case, allowing a reduction in activation free energy substantially beyond that provided by the common features mentioned above, are fairly clear from a physical point of view. The burial of the neutral Lys67 in the protein interior, in which the ammonium group nitrogen acts as an acceptor to the hydrogen on the tyrosine hydroxyl group, is a highly unusual structure, which presumably is forced in part by the geometry of the active site. This structure facilitates activation of the Tyr150 oxygen, which in turn is then able to activate W402. The positively charged Lys315 complements this chemistry, providing optimal electrostatic stabilization of maximal negative charge on the Tyr150 oxygen. In addition, the entire hydrogen bonded network of W418, W383, W401, Glu272, and Arg148 further concentrates, via polarization effects, positive charge in the atoms of Lys315 closest to Tyr150 and is thus optimally configured to produce a low barrier to hydrolysis. Presumably, this network was developed via evolutionary pressure to reduce the barrier so as to provide improved protection against β-lactam antibiotics.

By comparing with results from the R61 calculations in which Tyr159 is deployed as the general base, we can quantitatively decompose the contributions of various features of P99 to the stabilization of the transition state. We focus here on the models in which Tyr159/150 in R61/P99 is fully deprotonated. The concerted models have similar activation barriers in both systems, and the decomposition is clearer for the former than the latter. Our first step is to extract a QM model, shown in Figure 11, from the active sites of R61 and P99 in which the tyrosine is deprotonated. The structures are frozen at the QM/MM transition states and capped with hydrogens, the positions of which are geometry optimized. For the atoms in this model, there is a one-to-one correspondence of residues between the two enzymes (e.g., Lys315 is not included in the model), and differences in activation energy can be attributed strictly to differences in the geometry of the common set of atoms. The activation free energy of the R61 model is 26.5 kcal/mol—very close to that of the QM/MM activation energy for that system—whereas the activation energy for the P99 model is 24.5 kcal/mol. The conclusions that can be drawn from this are as follows:

(1) The QM model captures the energetics of the full R61 system, but not of P99. The obvious reason for this is the exclusion of Lys315 and its associated hydrogen bonded chain (W418, W383, W401, Glu272, Arg148).

(2) The structures extracted from P99 and R61 are remarkably similar in both geometry and energy. The 2.0 kcal/mol difference is likely attributable to the difference in distance of the ester oxygen of Ser62/64 in R61/P99, which is significantly closer to the tyrosine in R61 than in P99, and would have the effect in this particular hydrogen bonding pattern of destabilizing additional charge on the oxygen, thus making it more difficult to pull the hydrogen off the catalytic water.

Next, we can examine the difference in activation barrier in both systems, starting from the deprotonated tyrosine structure (and, for this purpose, not considering the activation energy required to produce the deprotonated tyrosine structures from the acyl intermediate ground states). From Figure 8, we calculate this differential to be 3.0 kcal/mol. The physical interpretation of this difference is that Lys315 and its associated hydrogen bonded chain extract additional charge density from the tyrosine ring out onto the oxygen. The pK_a of tyrosine (9.6)[84] is considerably lower than that of, for example, methanol (15.5) because some of the anion electron density can be delocalized into the benzene ring of the tyrosine. While this reduces the energy needed to extract a proton, it also diminishes the magnitude of the charge on the oxygen in the anion. The positively charged groups Lys67 and Lys315 in P99 counteract this effect and concentrate charge on the oxygen atom where it is needed to extract the hydrogen. Lys65 performs a similar function in R61, but obviously two such groups (one of which is further polarized by its hydrogen bonding chain) is substantially more effective than one.

To demonstrate the correctness of this hypothesis, we have determined electrostatic potential (ESP) fit charges for the deprotonated tyrosine structures from the two species. The ESP charges on the tyrosine oxygens are -0.45 and -0.47 in R61 and P99, respectively, and confirm the picture of the charge distributions discussed above. The assertions concerning the greater effectiveness of a higher concentration of charge in the abstracting atom are more difficult to unambiguously illustrate via a simple calculation. From a physical point of view, the argument is clearly plausible. The electrostatic interaction at the transition state, where the hydrogen being abstracted already possesses a nontrivial positive charge, will be enhanced by a considerable margin by increasing the negative charge on the oxygen atom which is closest to the hydrogen. Furthermore, it is difficult to find an alternative explanation for the large reduction in the barrier height in the P99 system. Finally, from the above analysis we can extract the stabilization of the P99 barrier that can be attributed to Lys315 and the members of its hydrogen bonded chain. The total amounts to 1.0 kcal/mol (the difference between the R61 and P99 activation energies versus the deprotonated tyrosine acyl intermediates, minus the 2.0 kcal/mol already attributed to intrinsic differences in the structure of the common residues).

The last contribution to the activation barrier is the free energy required to deprotonate the tyrosine. This value is 15.5 kcal/

(84) Nozaki, Y.; Tanford, C. *Methods Enzymol.* **1967**, *11*, 715–734.

mol higher in the R61 system than in P99. The reason for this large differential, namely the lack of a third hydrogen bond donor in the first coordination shell of the tyrosine oxygen in R61, has been discussed in detail above. When all three contributions are summed, a very large difference in activation energy is obtained. We have hypothesized that the R61 system to some extent overcomes this by relying on the alternative mechanism of using Lys65 as a general base (else the experimentally observed barrier height would be ~40 kcal/mol, not 27[25]). However, as has been discussed above, this is quantitatively inferior to the tyrosine mechanism when the latter has a suitable electrostatic environment.

Of significant interest is whether this picture is consistent with some of the key mutation experiments that have been carried out on the P99 system. While detailed computations of rate constants for the mutant species (which we do not report in the present paper) are the only way to interrogate the quantitative performance of the model, we can at least consider whether these experiments are qualitatively consistent with the proposed picture of the catalytic mechanism. The first such mutation to consider is one in which Lys315 is changed to His.[75] This results in a significant, but not catastrophic, reduction in the hydrolysis rate, corresponding to a ~3.5 kcal/mol elevation of the free energy barrier. This result can readily be explained by assuming that, upon mutation, either reorganization of the protein side chains or incursion of water molecules would result in a replacement for the Lys315 hydrogen bond to the Tyr150 oxygen, thus at least retaining a full complement of hydrogen bonds in the first coordination shell. While the replacement group (whether water or an uncharged amino acid) is not as good as a lysine at stabilizing negative charge on the tyrosine oxygen (which presumably is why the lysine was evolutionarily selected for its position), it is nowhere near as bad as positioning the ester oxygen in this location, which is in effect what happens in R61. Note also that if one mutates only Lys315, Glu272 is still present to polarize the resulting donor species. Viewed in this fashion, the experimental results are not inconsistent with the current calculations (although whether our calculations will be able to quantitatively reproduce the mutant barriers remains to be seen).

A second mutation to consider is that of Glu272 to Val.[26] Again, one has to ask what happens to the structure if such a mutation is made. Presumably, the valine side chain would if possible avoid contact with Lys315, and other groups (most likely waters) would instead make hydrogen bonds with the Lys315 hydrogens. Although no single group would adequately replace a charged oxygen, it seems likely that two hydrogen bonds could be formed to waters. This would be competitive with the salt bridge formed by Glu272. This scenario is consistent with the 1.3 kcal/mol increase in activation barrier observed experimentally for this mutation.

Another mutation is that of Lys67 to Arg, which leads to a 2−3-fold reduction in deacylation rate.[77,85] The small effect upon the activation energy (an increase of 0.4−0.6 kcal/mol) can be rationalized by considering the role of Lys67 in the P99 deacylation mechanism. Both arginine and lysine are basic residues capable of stabilizing deprotonated Tyr150. However, the distributed nature of the positive charge over the arginine side chain terminus would lead to a slightly weaker interaction with Tyr150 versus that seen with Lys67.

Finally, the mutation of Tyr150 itself produces significant reductions in the reaction rate,[26,30] which is consistent with its key role as a general base. Mutation of the tyrosine to either phenylalanine or serine results in a $\sim10^4$ reduction in deacylation rate when cephalothin is the ligand, corresponding to an activation energy increase of ~6 kcal/mol. This is still a substantially higher rate of deacylation than is observed in the R61 system, presumably because whatever replaces Tyr150 as the general base (e.g., Lys67), while not as effective, benefits from the electrophilic environment available in P99. However, a detailed picture of the hydrolysis reaction in this (and other) mutant enzymes will require explicit calculations.

We next turn to the central question posed at the beginning of this paper. What are the structural features responsible for the huge difference in hydrolysis rates between the P99 and R61 enzymes? From the discussion above, it appears to be extremely difficult to reduce the activity of the β-lactamase to anything approaching the levels of the PBP, other than by replacing the tyrosine general base. The answer to the question just posed is implicit in the discussion we have presented previously concerning the electrostatic environment of Tyr159 in R61. If the cephalothin ligand were not blocking the first coordination shell of the tyrosine in R61 (Figure 6), then water molecule(s) and/or His298 would be able to hydrogen bond to the tyrosine oxygen. It seems reasonable to hypothesize that the then more favorable electrostatic environment around Tyr159 would facilitate its function as a general base and lead to a hydrolysis rate much closer to that of the β-lactamase. Indeed, peptide substrates are hydrolyzed quite efficiently by PBPs. Unfortunately, there are no cocrystallized structures of acyl-enzyme intermediates for such substrates.

The conclusion is therefore that it is the ability of the β-lactamase to accommodate cephalothin (and presumably other β-lactam antibiotic ligands) without elimination of the Lys315 hydrogen bond to the Tyr150 hydroxyl that is the key to its efficient hydrolytic activity. This accommodation is very likely due to the deeper active site pocket, and associated positioning of key residues that hydrogen bond with the ligand, as compared to the PBP. The specific presence of Lys315 appears not to be strictly necessary, since the Lys315 mutant is still many orders of magnitude more active than a PBP (although quantitatively diminished in activity from the wild type).[75] Presumably, the ligand would only have to displace water molecules in the mutant if it were to press up against Tyr150 in the same fashion as is observed in the cocrystallized cephalothin-R61 structure. The fact that it fails to do so suggests that such proximity is energetically unfavorable, and occurs in the PBP only because of geometrical constraints. In making the other interactions needed for binding in the active site cavity, the ligand is forced to occupy what certainly appears to be a rather surprising (and probably energetically unfavorable) space proximate to the tyrosine, without making particularly effective hydrogen bonding interactions. This structural motif, in turn, is the source of the efficacious antibiotic activity of cephalothin (and quite likely other β-lactam antibiotics).

It is important to note that our conclusions are dependent in part upon the structure we obtained from docking cephalothin

(85) Tsukamoto, K.; Tachibana, K.; Yamazaki, N.; Ishii, Y.; Ujiie, K.; Nishida, N.; Sawai, T. *Eur. J. Biochem.* **1990**, *188*, 15−22.

into the P99 active site. At the time this docking was carried out, the arguments concerning hydrogen bonding of multiple groups to Tyr150 were not at all understood, so the structure was obtained in a completely unbiased fashion, and ultimately optimized by molecular mechanics and QM/MM methods. It is of course possible that this structure is incorrect. However the straightforward accommodation of the ligand to the active site without exertion of undue strain, and the agreement of the computed free energy of activation with experiment, suggest otherwise. In addition, comparison with the rapidly hydrolyzed acyl-enzyme intermediate formed between amoxicillin and the *Escherichia coli* AmpC β-lactamase[86] shows that ligand to be bound in a nearly identical manner to that achieved in the docked structure of cephalothin in P99. Nevertheless, this issue needs to be examined more extensively. Similarly, the precise geometric and energetic reasons for the crowded R61/cephalothin structure should be further elucidated.

The evolutionary pathway for creation of a class C β-lactamase from a PBP then seems clear. Mutation of residues in the active site cavity (as well as those controlling the size and shape of that cavity, which are not necessarily the same) have evolved to alter the geometry so as to reposition the antibiotic ligands into a more favorable location. At the same time, the ligands themselves were no doubt evolving so as to increase their efficiency in blocking the tyrosine. Understanding the details of how the geometry is shifted, beyond obvious observations concerning cavity size, is far from trivial and we intend to explore this issue in a subsequent publication. Nonetheless, we believe that the basic physical picture presented here—which, to our knowledge, has not been previously recognized—is essential to the understanding of the interactions of β-lactam antibiotics with both PBPs and β-lactamases, which, assuming that the calculations and analysis above are in essence correct, can now be put forth on a both a quantitative and physically intuitive basis.

V. Conclusion

We have modeled the deacylation reaction for the β-lactam antibiotic cephalothin bound to both a PBP (*Streptomyces* sp. R61 DD-peptidase) and a class C β-lactamase (cephalosporinase from *Enterobacter cloacae* P99), using accurate, large-scale QM/MM computations. Good quantitative agreement with experimental data for hydrolysis was obtained for P99, and a novel and satisfying physical explanation was elucidated as to why the β-lactamase is qualitatively more efficient at carrying out hydrolysis than the PBP. This explanation, in addition to deriving detailed support from the QM/MM results, is qualitatively consistent with the otherwise puzzling effects of site-directed mutagenesis on the hydrolysis rate constant.

The work reported above provides a solid foundation on which to attempt more ambitious objectives. These include the following:

(1) Quantitative modeling of the reaction rate in R61. Our initial efforts will be directed toward the Lys65 mechanism as discussed above, but, if this proves to be infeasible, we will have to consider other as yet undiscussed alternatives.

(2) Quantitative prediction of the changes in rate constant due to site-specific mutation. This will require prediction of the modified protein structures. We have been developing methods capable of accomplishing this,[82,83] which can be calibrated via side chain predictions for available crystal structures.

(3) Design of new β-lactam antibiotics, and compounds capable of inactivating β-lactamases. The ability to reliably compute the deacylation reaction rate, as well as (presumably) any other reactions that might occur between the enzyme and substrate in the active site, indicates potential for the virtual design of novel compounds with improved properties. An obvious first step in this direction is to model the interaction of an irreversible β-lactamase inhibitor such as clavulanic acid with a β-lactamase, investigating the reactions thought to be responsible for the irreversible inactivation.[87]

(4) Construction of a minimal cassette of mutations capable of converting a PBP into a β-lactamase, and vice versa. The physical picture of what controls the relative reaction rates, presented above, should be immediately helpful in achieving this goal. It is also feasible to test the effect of various mutations by computational means, using side chain prediction methods to generate new structures, docking methods to position the ligand in the cavity, and QM/MM methods to assess the hydrolysis rate of the mutant enzyme.

Acknowledgment. This work was supported by grant GM52018 from the NIH (to R.A.F.) and by grants from the Beckman Foundation and the NIH (RO1-GM62867) to V.W.C. V.W.C. is a recipient of a Beckman Young Investigator Award, a Burroughs Wellcome Fund New Investigator Award in the Toxicological Sciences, a Camille and Henry Dreyfus New Faculty Award, and a NSF CAREER Award. Computational resources were provided by NPACI (to R.A.F.). This research was performed in part using the Molecular Science Computing Facility (MSCF) in the William R. Wiley Environmental Molecular Sciences Laboratory at the Pacific Northwest National Laboratory. We acknowledge support from the US Department of Defense through an NDSEG Fellowship to B.F.G. and from the NIH through a Biophysics Training Grant to B.F.G.

Supporting Information Available: Figures S1, S2 (PDF). This material is available free of charge via the Internet at http://pubs.acs.org.

JA036879A

(86) Trehan, I.; Morandi, F.; Blaszczak, L. C.; Shoichet, B. K. *Chem. Biol.* **2002**, *9*, 971−980.

(87) Labia, R.; Barthelemy, M.; Peduzzi, J. *Drugs Exp. Clin. Res.* **1985**, *11*, 765−770.